04.1

Investigation of the influence of the type of the lightning diverter strip on the spectrum of electromagnetic interference on the antenna under the model of the nose radome of the aircraft by using an artificial thunderstorm cell

© A.G. Temnikov, L.L. Chernensky, A.V. Orlov, N.Y. Lysov, O.S. Belova, D.I. Kovalev, T.K. Kivshar

National Research University „MPEI“, Moscow, Russia
E-mail: TemnikovAG@mpei.ru

Received May 14, 2021
Revised July 13, 2021
Accepted July 26, 2021

The paper presents the results of physical modeling of the effect of solid and segmented lightning diverter strips on the spectrum of electromagnetic interference on the antenna under the model of the aircraft nose radome under the influence of an artificial thunderstorm cell. It is shown that the use of segmented lightning diverter strips leads to appearance of signals with frequencies up to a few gigahertz in the spectrum on the antenna. The relationship between the antenna signal spectrum and spectral characteristics of current pulses on the lightning diverter strip is established. The influence of discharges along the radome surface and those between the segments on the electromagnetic interference spectrum on the antenna under the radome has been revealed.

Keywords: lightning, solid and segmented lightning diverter strips, model of aircraft nose radome, artificial thunderstorm cell, wavelet spectrum, discharge.

DOI: 10.21883/TPL.2022.14.52058.18871

More than a third part of lightning strikes on an aircraft falls on its nose part where the dielectric nose radome is installed which is designed to protect the antenna systems of the radio navigation facilities against the environmental impacts in flying conditions [1–3]. For the nose radomes lightning protection, solid lightning diverter strips (rigid busbars) and segmented lightning diverters are mainly used [1,3–5]. Thunderstorm clouds and lightnings create on the radome surface discharges that can induce on the antenna interference signals of different spectra. The lightning electromagnetic field effect on the under-radome facilities occurs in a wide frequency band [6]. The most hazardous are the interferences involving frequencies close to the operating frequencies of the under-radome radar and related computing equipment. Such interferences may cause the navigation equipment malfunction and even emergencies [5,7,8].

Physical simulation with the artificial thunderstorm cell enables revealing possible specific effect of the type of the aircraft nose radome lightning protection (with solid or segmented lightning diverter stripes) on the spectrum of signals detected by the model antenna during formation of the discharge from the model lightning diverters over the radome surface and inside it. This will enable defining the key aspects of this effect and propose promising ways to correct the nose radome lightning protection so as to reduce the intensity of the interference signals induced on the antenna in the frequency band hazardous for the radio navigation facilities.

The effect of the lightning diverter stripe types on the spectrum of electromagnetic interference on the aircraft under-radome antenna was studied using models involving artificial negative-polarity thunderstorm cells at the experimental setup described in [9]. The nose radome models were fabricated from polyethylene-terephthalate in the form of the paraboloid of revolution. On their outer surface there were four solid (Fig. 1, *a*) or segmented (Fig. 1, *b*) model lightning diverter stripes. The models were mounted on the earthed electrostatic screen in the artificial thunderstorm cell electric field more than 1 MV in potential. Two versions of the segmented model lightning diverters differing in the gap Δd between the neighboring segments (Fig. 1, *b*) were considered. The under-radome radar antenna was simulated by a flat circular antenna 15 cm in diameter. For each type of the model lightning diverter strip, a series of experiments of no less than sixty sets was conducted in which discharge current from the model lightning diverter on the radome outer surface and interference signal induced on the under-radome model antenna were detected by using a digital storage oscilloscope (DPO 7254 with the analog transmission band of 2.5 GHz) with low-inductance coaxial shunts (resistance of 0.5 Ω, reproducibility of the rectangular nanosecond pulse from the G5-56 generator). To find spectral characteristics of the discharge current pulses and electromagnetic radiation induced by them, the experimental results were processed with a special-purpose program code based on the wavelet analysis. As the wavelet basis, the „Mexican Hat“ wavelet most often used in analyzing fast-evolving discharge processes was chosen [10]. This allows establishment at a selected time interval of the relation between the spectral characteristics of signals on the model antenna and parameters of the discharge from

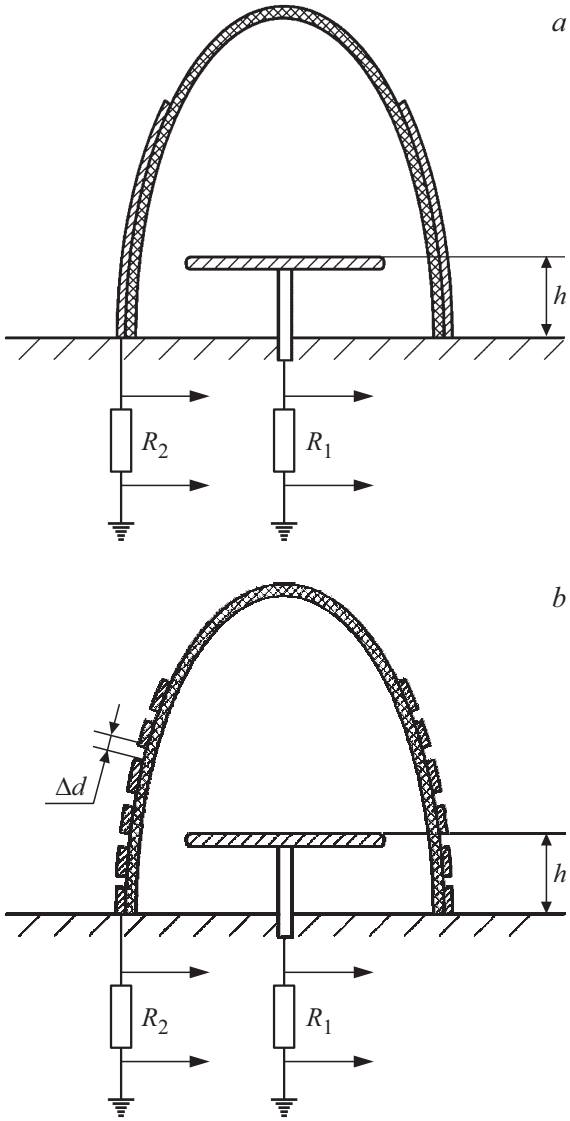

Figure 1. A model of an aircraft nose radome with solid (a) and segmented (b) electrodes on the radome outer surface.

the lightning diverter stripe on the outer surface of the aircraft model nose radome. In processing and analyzing the acquired spectra, the wavelet spectrum maximal frequency $f_{\max}$ and frequency $f(C_{\max})$ corresponding to the wavelet spectrum maximum intensity were determined. The experiments showed that at the same time the discharge between the artificial thunderstorm cell and solid lightning diverter strip is accompanied by formation of discharges over the model radome surface. „Reverse“ discharges might occur between the model antenna edge and radome shell under the action of charges deposited on the radome inner surface [9]. Typical oscilloscope records of current pulses of the discharge from the model solid lightning diverter stripe and interference signal induced on the model antenna jointly with the typical wavelet spectrum of the signal are presented in Figs. 2, a and b, respectively. When the segmented lightning diverter stripes are used, the priority scenario is formation of spark discharges in the gaps between the neighboring segments on the outer surface of the model dielectric radome. These discharges might be accompanied by surface discharges in the radome top part free of segmented electrodes, which ascended towards the artificial thunderstorm cell, and also by „reverse“ discharges between the antenna edge and radome inner surface. Typical oscilloscope records of current pulses of the discharge from the model segmented lightning diverter and of the interference signal induced on the under-radome model antenna, and the typical signal wavelet spectrum are given in Figs. 3, a and b, respectively.

Thus, both types of the lightning diverter strips did not excluded formation of a reverse discharge from the model antenna, which was several tens of amperes in amplitude. The presence of the oscillating component in the antenna signal oscilloscope record indicates a considerable

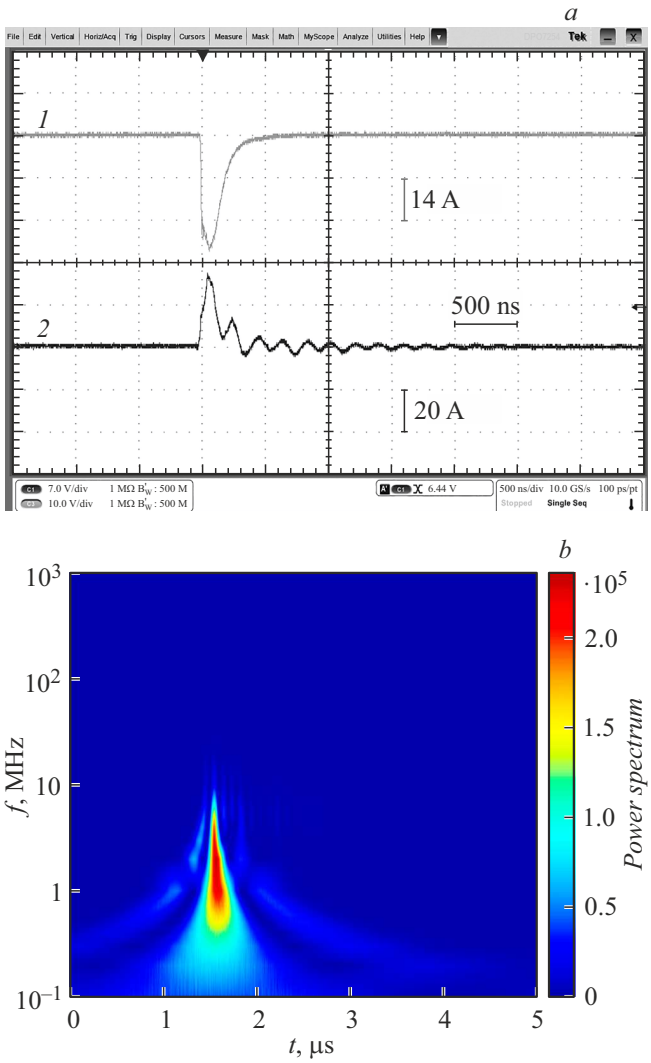

Figure 2. a — typical oscilloscope records of current pulses of discharge from the solid lightning diverter model (shunt 0.5 Ω) (*1*) and of signals on the antenna (shunt 0.5 Ω) (*2*); b — wavelet spectrum of electromagnetic interference detected with a flat antenna under the model radome.

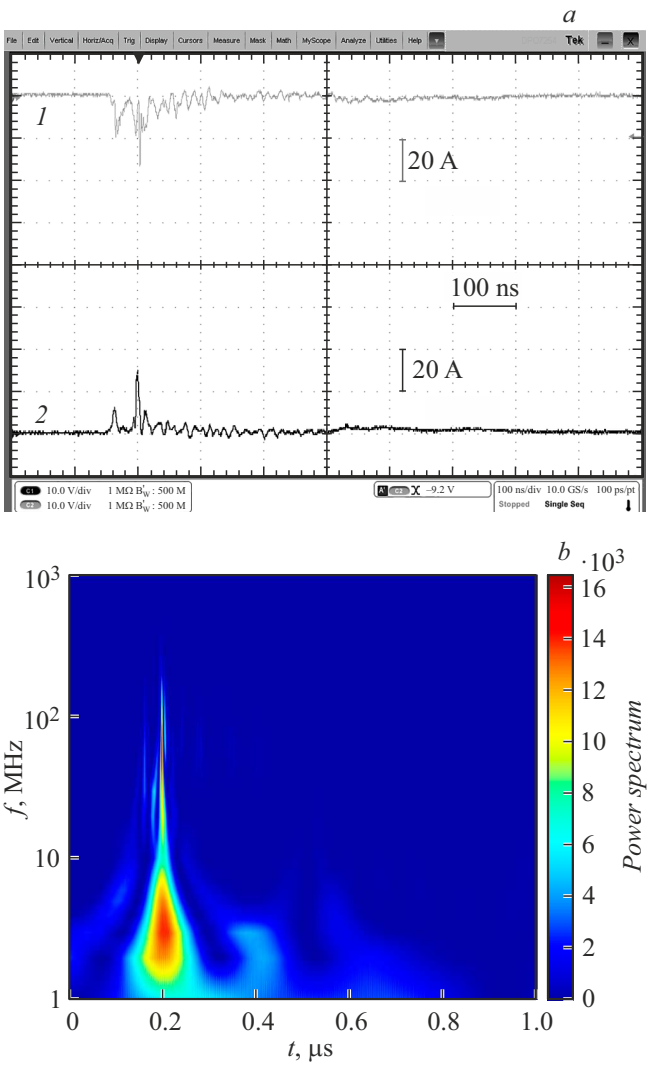

Figure 3. *a* — typical oscilloscope records of current pulses of discharge from the model segmented lightning diverter stripe (shunt 0.5 Ω) (*1*) and of signals on the antenna (shunt 0.5 Ω) (*2*); *b* — a wavelet spectrum of electromagnetic interference detected by a flat antenna under the model radome.

contribution to the signal from bias currents induced by the discharge between the artificial thunderstorm cell and model lightning diverter, as well as by discharges occurring over the radome due to accumulation of a considerable charge on its surface. The main parameters of current pulses of discharges from the model lightning diverters and those of signals induced by them on the under-radome model antenna belonged to the close ranges but average values for the solid lightning diverters were 10–60% higher.

Wavelet spectra of interference signals induced on the antenna under the aircraft model nose radome exhibited frequency characteristics essentially different for the protection versions with solid and segmented lightning diverters (Table 1). Maximal frequencies $f_{\max}$ in the antenna signal wavelet spectrum were in average an order of magnitude higher for the segmented lightning diverter stripes than for solid ones. A similar behavior was revealed also for frequency $f(C_{\max})$ corresponding to the wavelet spectrum maximal intensity. For the segmented lightning diverters, limiting values of $f_{\max}$ and $f(C_{\max})$ in the antenna signal wavelet spectrum reached 1.89 GHz and 610 MHz, respectively.

A similar tendency was exhibited by the wavelet spectrum of current pulses detected on the segmented and solid lightning diverter stripes (Table 2). Maximal frequencies $f_{\max}$ in the current pulse wavelet spectrum were in average 5 times higher for the segmented lightning diverters than for solid ones. Frequencies $f(C_{\max})$ corresponding to the maximal intensity of the current pulse wavelet spectrum were in average more than an order of magnitude higher for the segmented lightning diverters than for solid ones. For the segmented lightning diverter stripes, the current pulse limiting values of $f_{\max}$ and $f(C_{\max})$ reached 1 GHz and 350 MHz, respectively.

When the segmented lightning diverter stripes are used, a pronounced influence of distance between neighboring segments Δd on the spectral characteristics of interference signals induced on the under-radome model antenna was found out (Table. 1). Reduction of Δd from 3.5 to 1 mm caused a 1.5-times increase in the maximal frequencies $f_{\max}$ of the antenna signal wavelet spectrum (from 208 to 356 MHz), while frequencies $f(C_{\max})$ corresponding to the wavelet spectrum maximal intensity $C_{\max}$ grew in average by 3 times (from 29 to 87 MHz). A similar though less pronounced tendency manifested itself also for wavelet spectra of the current pulses detected at the segmented lightning diverter stripe (Table 2).

Thus, it was experimentally demonstrated for the first time that the lightning diverter type radically affects the spectrum of electromagnetic interferences on the antenna under the model aircraft nose radome. When the segmented lightning diverter stripes are used, on the outer surface of the aircraft nose radome there arise frequencies ranging

Table 1. Average values (range) of typical frequencies of the wavelet spectrum of signals detected at the under-radome antenna

Parameter	Lightning diverter type		
	Segment ($\Delta d = 1$ mm)	Segment ($\Delta d = 3.5$ mm)	Solid
$f_{\max}$, MHz	356 (7–1890)	208 (2–900)	20 (1.5–75)
$f(C_{\max})$, MHz	87 (1–610)	29 (0.1–600)	3.6 (0.3–45)

Table 2. Average values (range) of typical frequencies of the wavelet spectrum of current pulses detected at the lightning diverter on the radome surface

Parameter	Lightning diverter type		
	Segment ($\Delta d = 1$ mm)	Segment ($\Delta d = 3.5$ mm)	Solid
f_{max}, MHz	271 (10–900)	207 (2–1000)	55 (1.4–260)
$f(C_{\max})$, MHz	47 (1.5–70)	27 (0.2–350)	2.1 (0.2–20)

from hundreds of MHz to several GHz of the spectrum of interference signals induced on the under-radome antenna, which may be harmful for normal operation of the radio navigation devices [1,7]. One of the key factors affecting the spectrum of electromagnetic interferences on the under-radome antenna is formation of the radome surface spark discharges between the lightning diverter segments. The results obtained may be utilized in improving methods for protecting the aircraft nose radome and radio navigation equipment mounted under it against thunderstorm clouds and lightnings.

Financial support

The study was carried out at the National Research University „MPEI“ and was financially supported by the RF Ministry of Science and Higher Education in the scope of State Assignment (project № FSWF-2020-0019).

Conflict of interests

The authors declare that they have no conflict of interests.

References

[1] A. Hall, in 2005 *Int. Conf. on lightning and static electricity* (Seattle, USA, 2005), p. 118. DOI: 10.13140/RG.2.2.21467.82727
[2] N.I. Petrov, A. Haddad, G.N. Petrova, H. Griffiths, R.T. Waters, in *Recent advances in aircraft technology*, ed. by R.K. Agarwal (IntechOpen, 2012), p. 523. DOI: 10.5772/36634
[3] C. Karch, C. Paul, F. Heidler, in *2019 Int. Symp. on electromagnetic compatibility (EMC EUROPE)* (Barcelona, Spain, 2019), p. 650. DOI: 10.1109/EMCEurope.2019.8871944
[4] D. Yan-chao, X. Xiu, H.U. Pingdao, in *2017 Int. Symp. on electromagnetic compatibility (EMC EUROPE)* (Angers, France, 2017). DOI: 10.1109/EMCEUROPE.2017.8094806
[5] A. Vukovic, P. Sewell, T. Benson, IEEE Trans. Antennas Propagat., **68** (11), 7287 (2020). DOI: 10.1109/TAP.2020.2998169
[6] J.-P. Parmantier, F. Issac, V. Gobin, Aerospace Lab J., **5**, ALO5-10 (2012). https://aerospacelab.onera.fr/al5/indirect-effects-of-lightning-on-aircraft-and-rotorcraft
[7] P.R.P. Hoole, M.R.M. Sharip, J. Fisher, K. Pirapaharan, A.K.H. Othman, N. Julai, S.A. Rufus, S. Sahrani, S.R.H. Hoole, J. Telecommun. Electron. Comput. Eng., **9** (3-10), 1 (2017). https://journal.utem.edu.my/index.php/jtec/article/view/3145
[8] P.R.P. Hoole, J. Fisher, K. Pirapaharan, Al K.H. Othman, N. Julai, Aravind CV, K.S. Senthilkumar, S.R.H. Hoole, Int. J. Control Theory Appl., **10** (16), 221 (2017). https://serialsjournals.com/abstract/39739_ch_22_f_ijcta_paper3.pdf
[9] A.G. Temnikov, L.L. Chernensky, A.V. Orlov, O.V. Polyakova, Pis'ma v ZhTF, **36** (18), 40 (2010) (in Russian).
[10] M.R.M. Esa, M.R. Ahmad, V. Cooray, J. Atmospher. Res., **138**, 253 (2014). DOI: 10.1016/J.ATMOSRES.2013.11.019